

SUPPORTING INFORMATION

3D Printing of Thermoreversible Polyurethanes with Targeted Shape-Memory and Precise In-Situ Self-Healing Properties

Yue Zhang, Xiang-Yu Yin, Mingyue Zheng, Carolyn Moorlag, Jun Yang, Zhong Lin Wang*

Table of contents

The supplementary information file includes, 8 supplementary Figures (Figures S1-S8), 1 supplementary Table (Table S1) and 4 supplementary videos (Video S1-S4).

Supplementary Figures	2
Fig. S1 FT-IR spectra	2
Fig. S2 ¹ H NMR spectra	2
Fig. S3 Solvent resistance	3
Fig. S4 TGA and DSC curves	3
Fig. S5 Photographs of printed samples and extruded ink filaments	3
Fig. S6 Consecutive shape memory cycles of PDAPU10	4
Fig. S7 UV-Vis-NIR spectra and temperature variation under IR irradiation	4
Fig. S8 Healing efficiencies of PDAPU10	4
Supplementary Table	5
Table S1 DSC results	5

Supplementary Figures

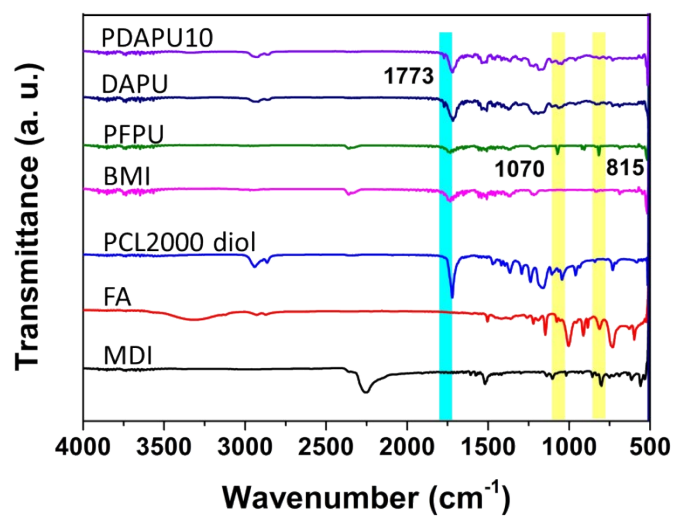


Fig. S1. FT-IR spectra of MDI, FA, PCL2000-diol, BMI, PFPU, DAPU and PDAPU10.

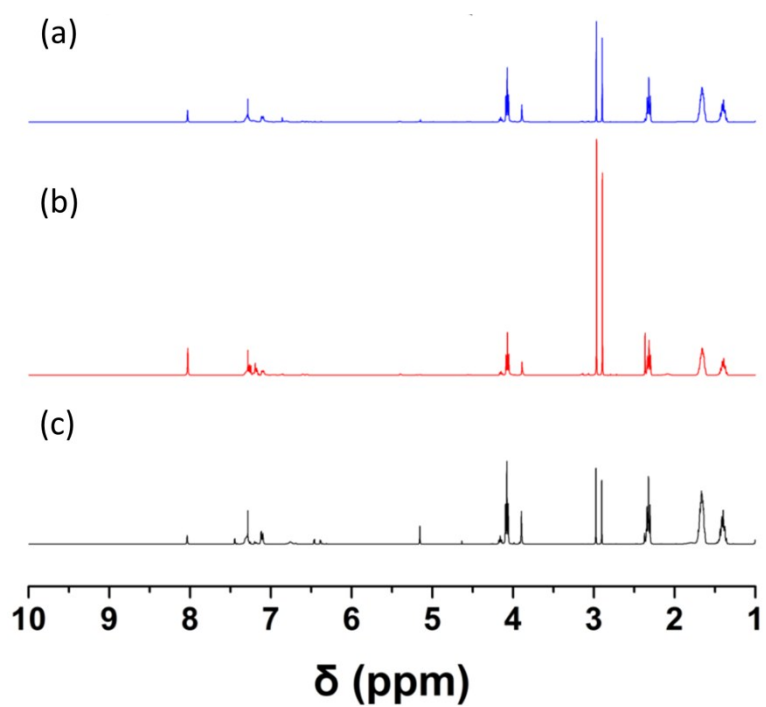


Fig. S2. ^1H NMR spectra of a) PDAPU10, b) DAPU and c) PFPU.

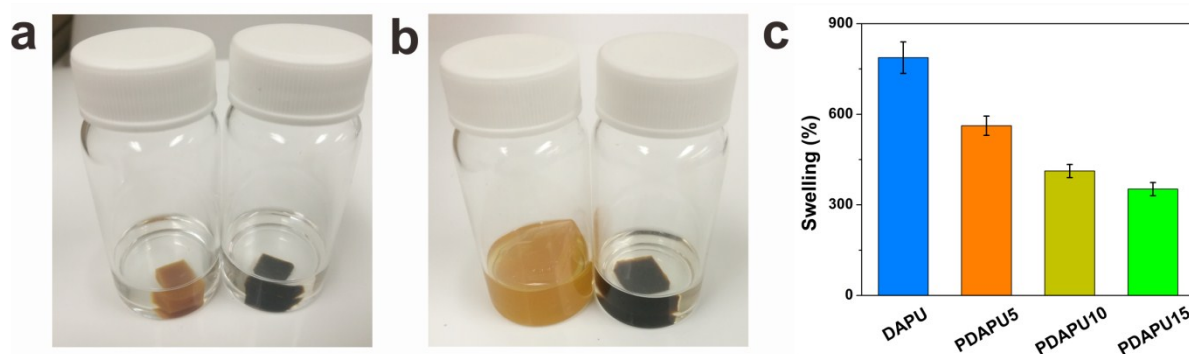


Fig. S3. Photographs of DAPU (brown) and PDAPU10 (brownish black) (a) before and (b) after being immersed in DMF for 24 h at room temperature. c) Swelling ratio for DAPU and PDAPUs at room temperature.

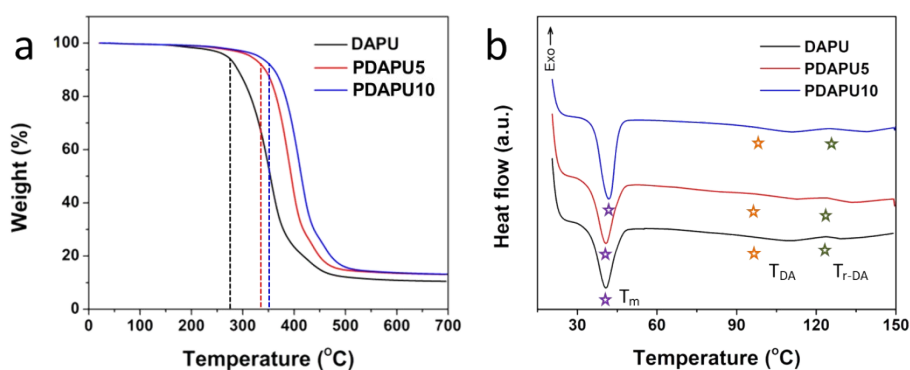


Fig. S4. a) TGA and (b) DSC curves of DAPU, PDAPU5 and PDAPU10. The TGA curves in Figure S4a exhibit the maximum degradation temperatures is 275.5 °C, 335.9 °C and 351.2 °C for DAPU, PDAPU5 and PDAPU10, respectively. Generally, the higher the cross-link degree, the more thermally stable the material. Clearly, the thermal stability of PDAPUs is higher than the DAPU, indicating that the AT could act as crosslinking agents to further improve the stability of the PDAPU.



Fig. S5. Photographs of samples printed from (a) DAPU and (b) PDAPU10. (c) The ink filaments extruded from DIW printer with different nozzle diameters. The inner diameter of 14#, 16#, 18# and 20# nozzles is 1.6 mm, 1.2 mm, 0.84 mm and 0.64 mm, respectively. The ink filament diameter is approximately equal to the nozzle size.

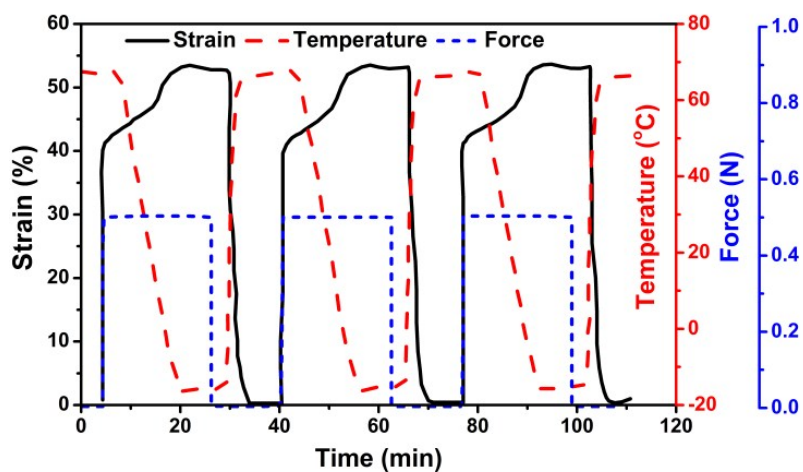


Fig. S6. Consecutive shape memory cycles of PDAPU10.

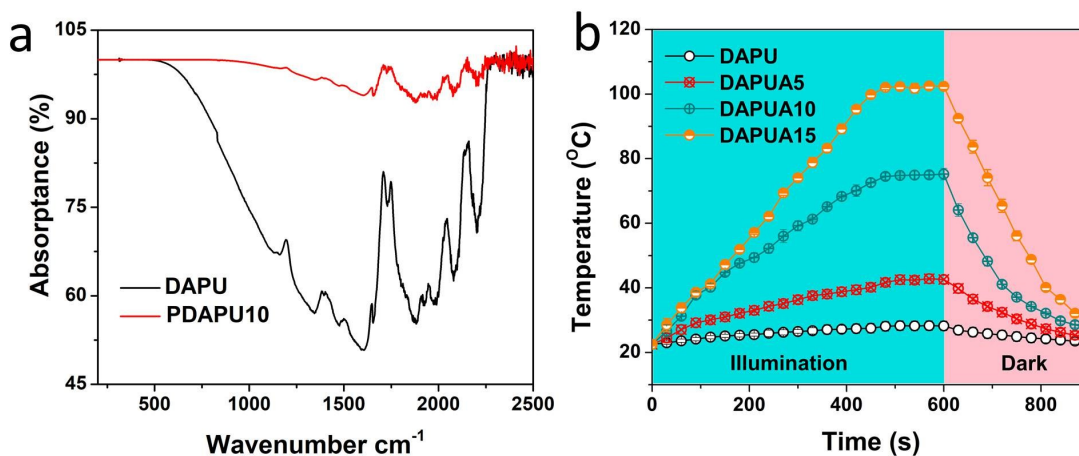


Fig. S7. (a) UV-Vis-NIR absorbance spectra of DAPU and PDAPU10. (b) IR-triggered temperature changes of DAPU, PDAPU5, PDAPU10 and PDAPU15.

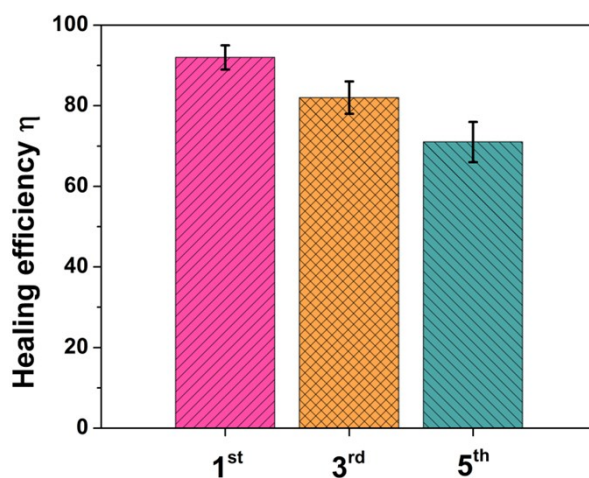


Fig. S8. Healing efficiencies of PDAPU10 for the first, third and fifth healing tests.

Supplementary Table

Table S1. DSC results for DAPU, PDAPU5 and PDAPU10.

	T_m (°C)	T_{DA} (°C)	T_{I-DA} (°C)
DAPU	41.7 ± 2.02	96.7 ± 2.21	124.7 ± 2.66
PDAPU5	42.8 ± 1.80	95.5 ± 1.53	126.4 ± 1.88
PDAPU10	44.9 ± 2.20	97.3 ± 2.36	127.8 ± 2.08